

Oral administration of nanostructured strontium-substituted hydroxyapatite for bone regeneration

Iorrana Índira dos Anjos Ribeiro^{1*}, Guillermo Alberto López², Aryon de Almeida Barbosa Júnior³, Alexandre Malta Rossi⁴, José Antônio Menezes Filho⁵, Fúlvio Borges Miguel¹, Fabiana Paim Rosa¹

¹Universidade Federal da Bahia, Instituto de Ciências da Saúde,

Laboratório de Bioengenharia Tecidual e Biomateriais, Salvador, BA, Brazil

²Instituto Federal de Educação, Ciência e Tecnologia da Bahia, Salvador, BA, Brazil

³Instituto de Patologia Geral e Cutânea, Salvador, BA, Brazil

⁴Centro Brasileiro de Pesquisas Físicas, Rio de Janeiro, RJ, Brazil

⁵Universidade Federal da Bahia, Faculdade de Farmácia, Laboratório de Toxicologia Clínica, Ambiental e Ocupacional, Salvador, BA, Brazil

Abstract

The objective was to evaluate the effect of oral administration of strontium (Sr) on the regeneration of a critical bone defect. Twenty Wistar rats were divided into two groups, assessed at 15 and 60 days postoperatively: GSr – oral administration of Sr; and CG – without oral administration of Sr. At 15 and 60 days, blood was collected to measure Sr and calcium (Ca), and the calvaria was removed for histomorphological and histomorphometric analyses. Sr²⁺ plasmatic concentrations were higher in GSr than in CG. The dosage of Ca²⁺ showed a small increase in the CG about the GSr. In all evaluated groups, new bone formation was restricted to the edges of the defect, and the residual area was filled with fibrous connective tissue. The oral administration of Sr associated with HA microspheres substituted by the metal, in a concentration of 23 mol%, did not affect the formation of the osteoid matrix.

Keywords: bone regeneration, hydroxyapatite, oral administration, rat, strontium.

INTRODUCTION

Strontium (Sr) is an alkaline earth metal, belonging to group 2A of the periodic table and with atomic number 38, found in the oceans, groundwater, earth's crust, and the human body. In the latter, it is considered a trace element present in plasma, extracellular fluid, and soft tissues, but the greatest deposition occurs in bones and teeth. Leafy vegetables, grains, seafood, and dairy products are food sources of this ion; however, its absorption is approximately 25 to 30% of the total intake [1, 2].

Despite the available studies, the physiological action of this metal is still the source of several studies focused on different clinical applications. However, it is already known that this ion has similarities in size, charge, site and form of absorption, site of deposition, and excretion with calcium (Ca). Thus, it presents similar chemical and physical properties that justify its biological role like Ca in some mechanisms, such as muscle contraction, blood coagulation, and secretion of hormones, in addition to its action and incorporation in bone tissue [2-5].


The correlation between the use of Sr with increased regenerative capacity of bone tissue has been increasingly researched, with greater emphasis after the development of the drug strontium ranelate (SrRan) that began to be used

in the treatment of osteoporosis to increase bone mineral density [5, 6]. This drug has a dual action on the cells of this tissue, due to Sr stimulating two different mechanisms: 1) on osteoblasts, with inhibition of apoptosis and promotion of proliferation and differentiation of these cells, which favors the synthesis of the new bone matrix; 2) on osteoclasts, due to limitation in cell formation and differentiation, as well as stimulation of apoptosis, with consequent reduction of bone resorption [1, 5, 7, 8].

In addition to its use in individuals with osteoporosis, studies have investigated the effect of SrRan on the repair of critical [9-11] and non-critical [12-15] in animal models, with favorable results for bone neoformation. Despite the already proven benefits, the use of this drug has been restricted to individuals with severe osteoporosis and who have no possibility of treatment with other drugs, because the use of SrRan has been correlated with the risk of developing heart disease [2, 16]. With this, evaluating the association of Sr with biomaterials for application in bone defects, in non-osteoporotic animals, has gained prominence, likewise its application, through oral administration, as a pharmacological alternative in stimulating bone regeneration.

In this context, hydroxyapatite (HA) becomes a promising material, since it allows, during synthesis, the replacement of Ca in its structure by metals such as zinc (Zn) [17], Sr [18-22] and magnesium (Mg) [23]. Furthermore, according to Li et al. [24], the joint administration of Sr and Ca favors the expression of osteogenesis-stimulating genes and bone neoformation. Thus, using this ceramic as a Sr carrier

* indiraanjos@gmail.com

 <https://orcid.org/0000-0002-9602-1708>

shows to be an effective alternative for releasing these ions after oral administration. This occurs because when HA is synthesized by the principles of nanoscience, this material presents greater solubility, modifications in porosity, and reduction of particle size, which consequently increases the surface area, biodegradation, and bioabsorption [25, 26].

Nanostructured HA replaced with Sr (nSrHA) can be used locally to provide the direct release of Sr in the implantation region and, in these cases, also act as a scaffold, which provides a three-dimensional structure that enables the cellular events involved in tissue repair; or orally, to release this metal systemically. Thus, this study aimed to analyze the effect of oral administration of Sr, carried out using nanostructured HA, on the regeneration of critical bone defects in non-osteoporotic rats.

MATERIALS AND METHODS

Synthesis and characterization of strontium-substituted HA: strontium-substituted nanostructured HA (nSrHA) used in this study was produced and characterized at the Brazilian Center for Physics Research (CBPF), Rio de Janeiro (RJ), Brazil. The nanometric SrHA powder was synthesized by the wet precipitation method, using solutions of calcium nitrate [$\text{Ca}(\text{NO}_3)_2 \cdot 4\text{H}_2\text{O}$], strontium nitrate [$\text{Sr}(\text{NO}_3)_2 \cdot 6\text{H}_2\text{O}$], and dibasic ammonium phosphate [$(\text{NH}_4)_2\text{HPO}_4$]. A solution containing calcium nitrate and strontium nitrate (0.2M concentration) was dripped onto a dibasic ammonium phosphate solution, using a peristaltic pump with a flow rate of 4.5 mL/min, with a concentration

of 0.2M, maintaining pH 9 was achieved with concentrated ammonium hydroxide (NH_4OH), at a temperature of 90°C and mechanical stirring at 240 rpm. During this process, Sr was replaced in the HA structure by the addition of strontium nitrate at a concentration of 50%. After dripping, the mixture remained in digestion for 3h under the same conditions, with subsequent filtration in a Buckner funnel and resuspension in Milli Q water at 90°C until pH 7 was obtained in the washing water. The solid obtained was freeze-dried for 24h, macerated, and separated using a sieve with an opening $< 74\mu\text{m}$ mesh. To obtain microspheres, the nSrHA powder was added to the sodium alginate solution, in a 15:1 ratio, under slight agitation until a homogeneous paste was obtained, which was dropped into a solution of calcium chloride dihydrate ($\text{CaCl}_2 \cdot 2\text{H}_2\text{O}$, 0.15M) for the immediate formation of microspheres, which remained in this solution for 24 hours for complete gelation. After this, the material was washed in deionized water, dried in an oven at 60°C for 24 hours, separated according to the particle size range of 1 to 2 mm, and finally packed in appropriate bottles and sent for sterilization by gamma radiation.

The obtained material was characterized as to: i) surface area and pore size by the Brunauer-Emmett Teller (BET) method (Micromeritics ASAP 2020, Norcross, Georgia, United States); ii) chemical composition by Atomic Absorption Spectrometry (AAS) (Shimadzu AA 6800, Shimadzu Corporation®, Chiyoda, Tokyo, Japan); iii) crystallinity by X-ray diffraction (XRD) (HZG4, Zeiss®, Jena, Thuringia, Germany); iv) presence of functional groups by Fourier Transform Infrared Spectroscopy (FTIR)

Table I. Atomic absorption spectrometry of nSrHA microspheres.

Sample	Ca		P		Sr		Ca+Sr/P
	%m	mol	%m	mol	%m	mol	
nSrHA	16.20	0.40	15.00	0.48	23.00	0.26	1.38

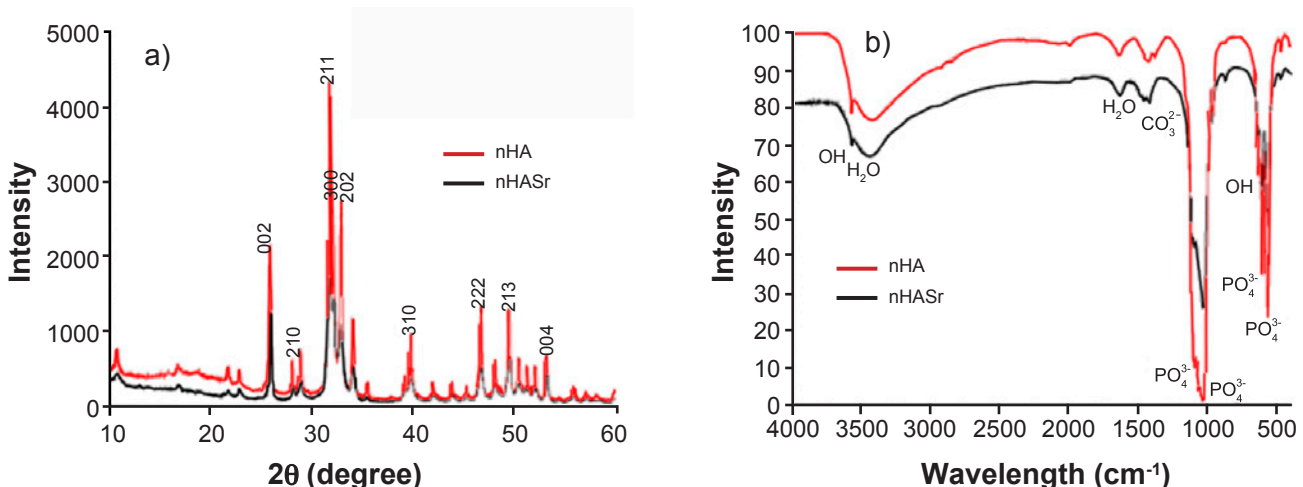


Figure 1: XRD and FTIR of nHASr and nHA. (A) XRD: It is noted that the bases of the main peaks of nHASr are slightly wider than those of nHA, which shows the lower crystallinity of HA with Sr. (B) FTIR: It is observed that both spectra show bands characteristic of HA – phosphate (PO_4^{3-}), hydroxyl (OH^{1-}) and water (H_2O).

(Schimadzu IR-Prestige 21, Shimadzu Corporation®, Chiyoda, Tokyo, Japan).

Regarding the analysis using the BET method, the surface area of the microspheres was 116.71 m²/g and the average pore width was 13.12 nm. The quantitative determination of the elements Ca, phosphorus (P), and Sr, as well as the Ca/P ratio of nSrHA microspheres, are presented in Table I.

In the XRD analysis, the diffractogram that the main peaks were wide, which shows the low crystallinity of the material (Figure 1A), concerning the standard PCPDFWIN 09.0432 (JCPDS – *Joint Committee on Powder Diffraction Standards*). FTIR revealed bands of phosphate ions characteristic of a HA, except in the regions 1438 cm⁻¹, 1365 cm⁻¹, and 870cm⁻¹, which indicate the presence of the carbonate ion, due to the alginate used during the processing of the microspheres (Figure 1B). The presence of the water bands in the FTIR spectrum proves that the microspheres were not heat-treated (Figure 1B).

Animals and surgical procedure: this study was approved by the Ethics Committee on Animal Use (CEUA) of the Health Science Institute (ICS) of the Federal University of Bahia (UFBA), protocol no. 063/2014. Twenty male Wistar rats, with an average weight of 375 g, aged 3 to 4 months, were randomly distributed into two experimental groups with five animals in each group and analysis period: GSr - empty bone defect associated with oral administration of Sr; CG - control group, empty bone defect, without oral administration of Sr, evaluated at biological points of 15 and 60 days postoperatively.

The confection of the critical bone defect with approximately 8.5 mm in diameter in the medial portion of the calvaria was performed similarly to that described in Miguel et al. [27] and illustrated in Santos et al. [28].

Oral administration of Sr: in the GSr, oral administration of Sr, at a dose of 900 mg/Kg/day, was performed by mixing microspheres with the animals' diet. For this, two pellets of the standard Nuvilab CR-1 feed (Nuvital, Quimtia®) were macerated and mixed with distilled water and the material. Then, this paste diet was placed in an appropriate container and offered to the animals from the 2nd to the 15th postoperative day. In the CG, the animals received the same

paste diet, however, without the addition of microspheres with Sr.

Biochemical analysis of Sr and Ca: the biochemical analyses were performed in the Laboratory of Clinical, Environmental, and Occupational Toxicology at the School of Pharmacy, UFBA. For the determination of the plasma concentration of Sr⁺² and Ca⁺² ions, 3.5 mL of blood was collected through transthoracic cardiac puncture at the 15 and 60-day biological points. The plasma Sr⁺² concentration was determined by graphite furnace atomic absorption spectrometry (GFAAS) according to the method described by D'Haese et al. [29] and the Ca⁺² concentration by Flame Atomic Absorption Spectrometry (FAAS), a method adapted from Welch et al. [30]. Statistical analysis of plasma Ca and Sr concentration was performed using the Wilcoxon Signed Ranks Test.

Histomorphological and histomorphometric analyses: at the biological time points of 15 and 60 days, after blood collection, the animals were euthanized by intraperitoneal lethal doses of ketamine and xylazine. Then, the upper portion of the calvaria was removed, the soft tissue was removed, and the specimen was fixed in 4% buffered formaldehyde for 72 h. Afterward, the samples were decalcified in 5% EDTA for seven days. After this, the calvaries were sent for routine histological processing, embedded in paraffin, and cut 5 µm thick. Histological sections were stained by hematoxylin-eosin (HE) and Masson Goldner's Trichrome (TG) and examined by common light microscopy. For histomorphometric analysis, *Leica Application Suite* (LAS) was used to quantify the percentage of the neoformed osteoid matrix (%OM) about the total defect area. The differences between the means obtained for each group/biological point were analyzed by the *Wilcoxon Signed Ranks Test*.

RESULTS

Biochemical analysis: the values of plasma concentrations of Sr⁺² and Ca⁺² found for the two experimental groups evaluated at 15 and 60 days are summarized in Table II. In this, it can be observed that in GSr the value of Sr⁺² was higher than in CG, at all points evaluated. On the other hand,

Table II. Plasma concentrations of Sr⁺² and Ca⁺² (mmol/L), mean (±SD, standard deviation), in GSr and CG, at biological points of 15 and 60 days.

Biological point	15 days		60 days		Wilcoxon Test
Groups	Sr ⁺²	Ca ⁺²	Sr ⁺²	Ca ⁺²	<i>p</i> value
GSr	0.0109 (±0.00091)	2.4518 (±0.06466)	0.0057 (±0.00187)	2.3901 (±0.14916)	Sr ⁺² <i>p</i> = 0.063 NS Ca ⁺² <i>p</i> = 0.438 NS
CG	0.0005 (±0.00006)	2.4971 (±0.03108)	0.0002 (±0.00003)	2.6019 (±0.05071)	Sr ⁺² <i>p</i> = 0.058 NS Ca ⁺² <i>p</i> = 0.063 NS
<i>p</i> value	<i>p</i> = 0.011 S	<i>p</i> = 0.151 NS	<i>p</i> = 0.009 S	<i>p</i> = 0.032 S	

NS: not significant; S: significant.

the plasma concentration of Ca^{+2} was higher at all biological points in the CG, when compared to the GSr. Throughout the experimental period, it was possible to notice that the concentration of Sr^{+2} decreased in both groups studied. On the other hand, Ca^{+2} levels decreased in the GSr and increased in the CG. The differences observed between the

values of plasma concentrations of Sr^{+2} at 15 and 60 days, as well as Ca^{+2} at 60 days, showed statistically significant differences when comparing GSr with CG.

Histomorphological analysis: at 15 days, both experimental groups showed osteoid matrix (OM) neoformation restricted to the bone borders and deposition

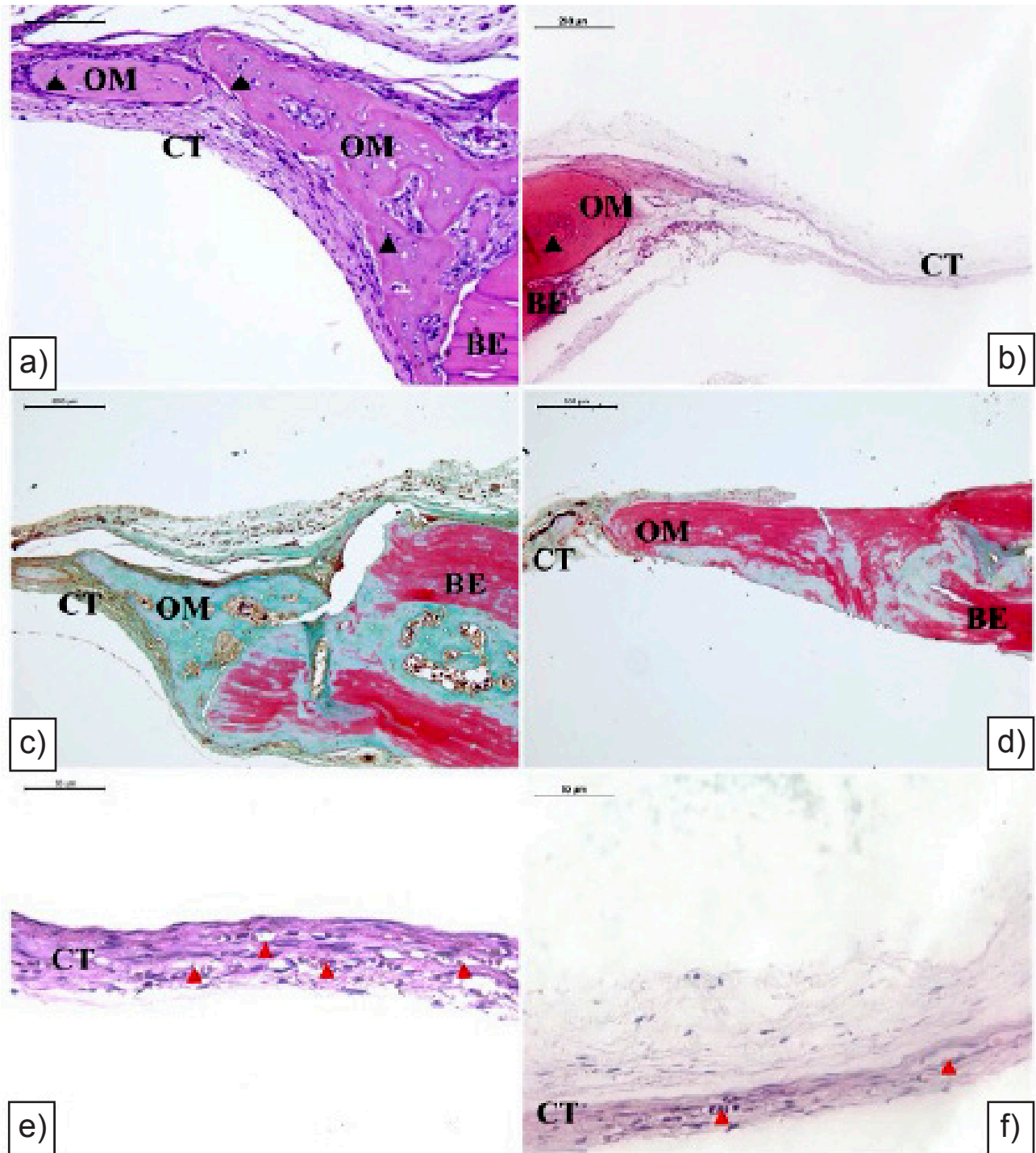


Figure 2: Photomicrographs of GSr at the 15 and 60 days biological point. Neoformed osteoid matrix (OM) is observed adjacent to the edge of the bone defect (BE); the presence of osteocytes (black arrow) and blood vessels (red arrow) in the connective tissue (CT). 15 days: (A) HE; (C) TG; and (E) HE. 60 days: (B) HE; (D) TG; and (F) HE.

of thin connective tissue (CT) in the remaining area of the defect (Figure 2A and 2C; Figure 3A and 3C). In the CG this tissue was thin and more organized than in the GSr (Figure 3E), in which the CT was loose and vascularized (Figure 2E). The inflammatory response seen at this biological point was chronic, and mild, with the presence of a predominantly

mononuclear inflammatory infiltrate dispersed in both groups (Figure 2A and 2E; Figure 3A and 3E). Vascular proliferation was more evident in GSr (Figure 2E).

At the 60-day biological point, OM neof ormation continued restricted to the bone defect borders, in both groups evaluated, however, with a more mature and organized aspect

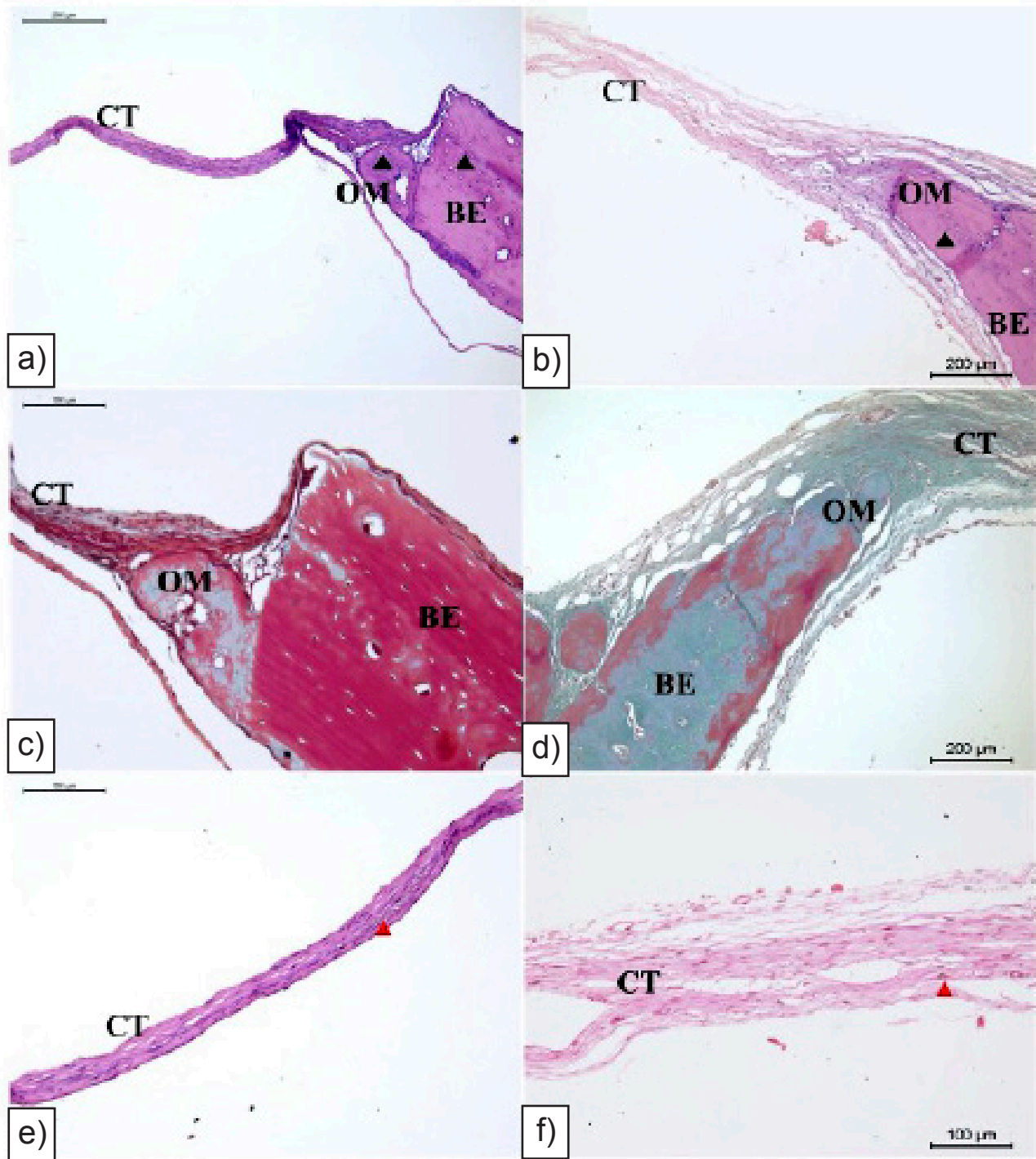


Figure 3: Photomicrographs of CG at the 15 and 60 days biological point. Note the presence of osteocytes (black arrow) in the newly formed osteoid matrix (OM) adjacent to the edge of the bone defect (BE); and blood vessels (red arrow) within the connective tissue (CT). 15 days: (A) HE; (C) TG; and (E) HE. 60 days: (B) HE; (D) TG; and (F) HE.

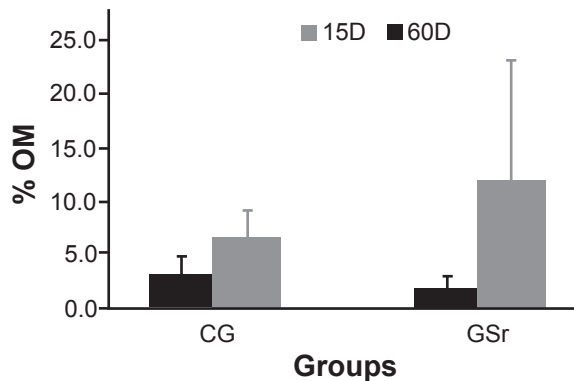


Figure 4: Percentage of newly formed OM (%OM) in the CG and GSr, in the two biological points.

about 15 days (Figure 2B and 2D; Figure 3B and 3D). In both groups, the residual area of the defect was filled by CT with a thickness smaller than the bone borders (Figure 2F; Figure 3F). At 60 days, chronic inflammation was regressive in both groups, but more evident in the GSr (Figure 2B and 3F; Figure 3B and 3F). In the GSr, the vascularization noted was less evident than at 15 days (Figure 2E and 2F), whereas in the CG, this finding was similar to that observed at 15 days (Figure 3E and 3F).

Histomorphometric analysis: the histomorphometric analysis showed, at 15 days, that the neoformation of OM was more evident in the CG and at 60 days this data was more evident in the GSr (Figure 4). However, the comparison by the Wilcoxon non-parametric test between the means obtained in the groups showed that the differences did not reach statistical significance in any of the biological points ($p > 0.05$).

DISCUSSION

Sr is a metal present in biological HA and with an important role in bone metabolism [5, 6], because it inhibits osteoblast apoptosis, which promotes the survival of these cells, besides increasing their proliferation and differentiation, due to the increased expression of osteogenic genes. Added to the stimulation of osteoblastic activity, this ion affects osteoclasts with the promotion of apoptosis and inhibition of proliferation and differentiation of these cells [1, 31, 32].

This ion has been used in the form of SrRan, in the treatment of osteoporosis [9, 16, 33] and associated with biomaterials for the repair of bone lesions [24, 34-36]. However, studies that propose the use of Sr systemically, for bone tissue regeneration, without being associated with ranelic acid, are scarce in the scientific literature. In this sense, this study was carried out with the perspective of collaborating with the development of an alternative method to the use of SrRan, considering its side effects and contraindications. Thus, this study evaluated the ability of Sr to stimulate bone regeneration when administered orally and carried by nanostructured HA.

In this study, bone neoformation was limited and restricted to the defect borders in both groups evaluated throughout the study. Although Sr acts positively on bone neoformation when administered orally, it is known that its action is directly related to plasma concentration, which depends on the dose administered and on metal absorption and bioavailability [2, 37].

Regarding absorption, factors correlated with the carrier, such as particle size, surface area, and porosity, also interfere with bioavailability, since they influence biodegradation when they encounter biological fluids [4, 38]. In this perspective, the HA used as Sr carrier in this study, was synthesized from nanometric powder and processed by using sodium alginate, to facilitate the degradation of the material and stimulate Sr release in the small intestine, the site where this ion is absorbed [2]. According to Loca et al. [39], the porosity of the biomaterial directly interferes with the release of drugs from the bioceramic, thus, the increase in porosity favored the faster release of the drug impregnated in the material.

However, even with these physicochemical characteristics that facilitate absorption, the biochemical results of this study showed a lower Sr plasma concentration, both at 15 (0.01088) and 60 days (0.00569), than that necessary to stimulate the formation of new bone matrix, according to Ammann et al. [40], which needs to be between 0.30 and 0.35 mmol/L of blood. This can probably be explained by the correlation between this metal and Ca, when administered together, since these ions compete for transporters and absorption sites, due to their similarity, which consequently interferes with absorption in a mutual manner [3, 41, 42]. Thus, when there is an increase in Sr supply, consequently, there will be a decrease in Ca uptake [3, 43]. This corroborates the biochemical results of this study since the Ca concentration was lower in the group treated with Sr than in the CG. It is worth mentioning that Ca has precise homeostatic control to regulate its body distribution [3, 32] since it participates in several physiological functions and activities, which possibly kept its blood values unchanged in both GSr and CG. Unlike Sr, which, probably due to the higher intake, exhibited higher plasma concentration in GSr when compared to CG.

According to Boivin et al. [44], animals treated with Sr present a heterogeneous distribution of this metal, with a greater presence in the newly formed bone, since, due to the lower mineralization, the exchange between Ca and Sr in HA crystals is facilitated. With the maturation of this tissue, the incorporation of Sr into the crystalline network becomes irreversible [5, 32, 44] which may have led to greater bone neoformation at 60 days in GSr.

In addition to the participation of micronutrients, it is known that bone regeneration depends on different factors such as angiogenesis, framework, size, and site of the lesion. In this study, the absence of a framework limited the neoformation of BM in both groups studied, even with the oral administration of Sr in the GSr. This occurs because the lack of three-dimensional support makes the

cellular and vascular events involved in bone regeneration unfeasible. In these cases, tissue repair occurs by fibrosis as demonstrated by Santos et al. [23], Miguel et al. [27], Miguel et al. [45], Santos et al. [28], and Ribeiro et al. [46]. In this tissue, in the neoformed connective tissue in the bone defect, it was possible to observe, in all groups evaluated, inflammatory response with infiltration of cells, predominantly, mononuclear, inherent to the tissue damage observed after the surgical procedure. The confection of the critical bone defect causes tissue injuries that cause blood extravasation and promote the local release of cytokines and inflammatory cells [47, 48]. Over time, the evolution of the inflammatory response stimulates osteoprogenitor cells from the periosteum to synthesize osteoid matrix, which is subsequently mineralized and transformed into the bone matrix, as observed at the edges of the defect in both groups studied.

Given the results found in this study, it is evident that the oral administration of Sr slightly increased the neoformation of OM throughout the experiment and that the dose, the plasma concentration, and the absence of a three-dimensional framework limited the complete regeneration of the bone defect. Thus, new studies are necessary to investigate the association of higher plasma concentrations of Sr with the presence of a three-dimensional framework implanted in the bone defect, in the search for a higher percentage of OM that preferably fills the entire defect area.

CONCLUSION

Under the experimental conditions of this study, it was concluded that the oral administration of Sr associated with HA microspheres substituted with the metal, at a concentration of 23 mol%, did not affect the formation of OM, due to the low plasma concentration of this ion.

REFERENCES

[1] Kołodziejaska B, Stepien N, Kolmas J. The Influence of Strontium on Bone Tissue Metabolism and Its Application in Osteoporosis Treatment. *Int J Mol Sci.* 2021;**22**(12):6564. doi:10.3390/ijms22126564.

[2] Borciani G, Ciapetti G, Vitale-Brovarone C, Baldini N. Strontium Functionalization of Biomaterials for Bone Tissue Engineering Purposes: A Biological Point of View. *Materials (Basel).* 2022;**15**(5):1724. doi:10.3390/ma15051724.

[3] Pors-Nielsen S. The biological role of strontium. *Bone.* 2004;**35**(5):583. doi:10.1016/j.bone.2004.04.026.

[4] Li H, Jiang F, Ye S, Wu Y, Zhu K, Wang D. Structures and physicochemical properties of vortioxetine salts. *Mater Sci Eng C Mater Biol Appl.* 2016;**62**:779. doi:10.1107/s2052520616010556.

[5] Querido W, Rossi AL, Farina M. The effects of strontium on bone mineral: A review on current knowledge and microanalytical approaches. *Micron.* 2016;**80**:122. doi:10.1016/j.micron.2015.10.006.

[6] Vegger JB, Brüel A, Sørensen TG, Thomsen JS. Systemic

Treatment with Strontium Ranelate Does Not Influence the Healing of Femoral Mid-shaft Defects in Rats. *Calcif Tissue Int.* 2015;**98**(2):206. doi:10.1007/s00223-015-0077-3.

[7] Bonnelye E, Chabadel A, Saltel F, Jurdic P. Dual effect of strontium ranelate: Stimulation of osteoblast differentiation and inhibition of osteoclast formation and resorption in vitro. *Bone.* 2008;**42**(1):129. doi:10.1016/j.bone.2007.08.043.

[8] Park J, Kang D, Hanawa T. New bone formation induced by surface strontium-modified ceramic bone graft substitute. *Oral Diseases.* 2015;**22**(1):53. doi:10.1111/odi.12381.

[9] Komrakova M, Weidemann A, Dullin C, Ebert J, Tezval M, Stuermer KM, Sehmisch S. The Impact of Strontium Ranelate on Metaphyseal Bone Healing in Ovariectomized Rats. *Calcif Tissue Int.* 2015;**97**(4):391. doi:10.1007/s00223-015-0019-0.

[10] Masalskas BF, Martins Júnior W, Leoni GB, Faloni APS, Marcaccini AM, Sousa YTCS, Castro-Raucci LMS. Local delivery of strontium ranelate promotes regeneration of critical size bone defects filled with collagen sponge. *J Biomed Mater Res A.* 2017;**106**(2):333. doi:10.1002/jbm.a.36237.

[11] Nahass HE, Din NNE, Nasry SA. The Effect of Strontium Ranelate Gel on Bone Formation in Calvarial Critical Size Defects. *Open Access Maced J Med Sci.* 2017;**5**(7):994. doi:10.3889/oamjms.2017.164.

[12] Buehler J, Chappuis P, Saffar JL, Tsouderos Y, Vignery A. Strontium ranelate inhibits bone resorption while maintaining bone formation in alveolar bone in monkeys (*Macaca fascicularis*). *Bone.* 2001;**29**(2):176. doi:10.1016/s8756-3282(01)00484-7.

[13] Rosa JA, Sakane KK, Santos KCP, Corrêa VB, Arana-Chavez VE, Oliveira JX. Strontium Ranelate Effect on the Repair of Bone Defects and Molecular Components of the Cortical Bone of Rats. *Braz Dent J.* 2016;**27**(5):502. doi:10.1590/0103-6440201600693.

[14] Miranda TS, Napimoga MH, De Franco L, Marins LM, Malta FS, Pontes LA, Morelli FM, Duarte PM. Strontium ranelate improves alveolar bone healing in estrogen-deficient rats. *J Periodontol.* 2020;**91**(11):1465. doi:10.1002/jper.19-0561.

[15] Matvieienko LM, Matvieienko RY, Fastovets OO. Effects of strontium ranelate on alveolar bone in rats with experimental diabetes mellitus. *Wiad Lek.* 2022;**75**(1):151. doi:10.36740/wlek202201201.

[16] Reginster J, Badurski J, Bellamy N, Bensen W, Chapurlat R, Chevalier X, Christiansen C, Genant H, Navarro F, Nasonov E, Sambrook PN, Spector TD, Cooper C. Efficacy and safety of strontium ranelate in the treatment of knee osteoarthritis: results of a double-blind, randomised placebo-controlled trial. *Ann Rheum Dis.* 2014;**51**(6):623. doi:10.1136/annrheumdis-2013-023388.

[17] Resende RFB, Fernandes GVO, Santos SRA, Rossi AM, Lima I, Granjeiro JM, Calasans-Maia MD. Long-term biocompatibility evaluation of 0.5% zinc containing hydroxyapatite in rabbits. *J Mater Sci Mater Med.* 2013;**24**(6):1455. doi:10.1007/s10856-013-4865-x.

[18] Calasans-Maia M, Calasans-Maia J, Santos S,

- Mavropoulos E, Farina M, Lima I, Lopes RT, Rossi AM, Granjeiro JM. Short-term in vivo evaluation of zinc-containing calcium phosphate using a normalized procedure. *Mater Sci Eng C Mater Biol Appl*. 2014;**41**:309. doi:10.1016/j.msec.2014.04.054.
- [19] Valiense H, Barreto M, Resende RF, Alves AT, Rossi AM, Mavropoulos E, Granjeiro JM, Calasans-Maia MD. In vitro and in vivo evaluation of strontium-containing nanostructured carbonated hydroxyapatite/sodium alginate for sinus lift in rabbits. *J Biomed Mater Res B Appl Biomater*. 2015;**104**(2):274. doi:10.1002/jbm.b.33392.
- [20] Machado CPG, Sartoretto SC, Alves ATNN, Lima IBC, Rossi AM, Granjeiro JM, Calasans-Maia MD. Histomorphometric evaluation of strontium-containing nanostructured hydroxyapatite as bone substitute in sheep. *Braz Oral Res*. 2016;**30**(1). doi:10.1590/1807-3107bor-2016.vol30.0045.
- [21] Carmo ABX, Sartoretto SC, Alves ATNN, Granjeiro JM, Miguel FB, Calasans-Maia J, Calasans-Mais MD. Alveolar bone repair with strontium-containing nanostructured carbonated hydroxyapatite. *J Appl Oral Sci*. 2018;**26**. doi:10.1590/1678-7757-2017-0084.
- [22] Li J, Yang L, Guo X, Cui W, Yang S, Wang J, Qu Y, Shao Z, Xu S. Corrigendum: Osteogenesis effects of strontium-substituted hydroxyapatite coatings on true bone ceramic surfaces in vitro and in vivo (2018 *Biomed Mater*. 13 015018). *Biomed Mater*. 2018;**13**(1):015018. doi:10.1088/1748-605x/ac64de.
- [23] Santos GG, Nunes VLC, Marinho SMOC, Santos SRA, Rossi AM, Miguel FB. Biological behavior of magnesium-substituted hydroxyapatite during bone repair. *Braz J Biol*. 2021;**81**(1):53. doi:10.1590/1519-6984.217769.
- [24] Li Y, Li Q, Zhu S, Luo E, Li J, Feng G, Liao Y, Hu J. The effect of strontium-substituted hydroxyapatite coating on implant fixation in ovariectomized rats. *Biomaterials*. 2010;**31**(34):9006. doi:10.1016/j.biomaterials.2010.07.112.
- [25] Ma PX. Biomimetic materials for tissue engineering. *Adv Drug Deliv Rev*. 2008;**60**(2):184. doi:10.1016/j.addr.2007.08.041.
- [26] Zhang W, Wang G, Liu Y, Zhao X, Zou D, Zhu C, Jin Y, Huang Q, Sun J, Liu X, Jiang X, Zreiqat H. The synergistic effect of hierarchical micro/nano-topography and bioactive ions for enhanced osseointegration. *Biomaterials*. 2013;**34**(13):3184. doi:10.1016/j.biomaterials.2013.01.008.
- [27] Miguel FB, Cardoso AKMV, Barbosa Júnior AA, Marcantonio Júnior E, Goissis G, Rosa FP. Morphological assessment of the behavior of three-dimensional anionic collagen matrices in bone regeneration in rats. *J Biomed Mater Res Part B Appl Biomater*. 2006;**78B**(2):334. doi:10.1002/jbm.b.30492.
- [28] Santos GG, Vasconcelos LQ, Poy SCS, Almeida RS, Barbosa Júnior AA, Santos SRA, Rossi AM, Miguel FB, Rosa FP. Influence of the geometry of nanostructured hydroxyapatite and alginate composites in the initial phase of bone repair. *Acta Cir Bras*. 2019;**34**(2). doi:10.1590/s0102-8650201900203.
- [29] D'haese PC, Landeghem GFV, Lamberts LV, Bekaert VA, Schrooten I, De Broe ME. Measurement of strontium in serum, urine, bone, and soft tissues by Zeeman atomic absorption spectrometry. *Clin Chem*. 1997;**43**(1):121. doi:10.1093/clinchem/43.1.121.
- [30] Welch MW, Hamar DW, Fettman MJ. Method comparison for calcium determination by flame atomic absorption spectrophotometry in the presence of phosphate. *Clin Chem*. 1997;**36**(2):351. doi:10.1093/clinchem/36.2.351.
- [31] Saidak Z, Marie PJ. Strontium signaling: Molecular mechanisms and therapeutic implications in osteoporosis. *Pharmacol Ther*. 2012;**136**(2):216. doi:10.1016/j.pharmthera.2012.07.009.
- [32] Marx D, Yazdi AR, Papini M, Towler M. A review of the latest insights into the mechanism of action of strontium in bone. *Bone Rep*. 2020;**12**:100273. doi:10.1016/j.bonr.2020.100273.
- [33] Yang S, Wang L, Feng S, Yang Q, Yu B, Tu M. Enhanced bone formation by strontium modified calcium sulfate hemihydrate in ovariectomized rat critical-size calvarial defects. *Biomed Mater*. 2017;**12**(3):035004. doi:10.1088/1748-605x/aa68bc.
- [34] Lin K, Liu P, Wei L, Zou Z, Zhang W, Qian Y, Shen Y, Chang J. Strontium substituted hydroxyapatite porous microspheres: Surfactant-free hydrothermal synthesis, enhanced biological response and sustained drug release. *J Chem Eng*. 2013;**222**:49. doi:10.1016/j.ccej.2013.02.037.
- [35] Lourenço AH, Neves N, Ribeiro-Machado C, Sousa SR, Lamghari M, Barrias CC, Cabral AT, Barbosa MA, Ribeiro CC. Injectable hybrid system for strontium local delivery promotes bone regeneration in a rat critical-sized defect model. *Sci Rep*. 2017;**7**(1):5098. doi:10.1038/s41598-017-04866-4.
- [36] Offermanns V, Andersen OZ, Riede G, Sillassen M, Jeppesen CS, Almqvist KP, Talasz H, Öhman-Mägi C, Lethaus B, Tolba R, Kloss F, Foss M. Effect of strontium surface-functionalized implants on early and late osseointegration: A histological, spectrometric and tomographic evaluation. *Acta Biomater*. 2018;**69**:385. doi:10.1016/j.actbio.2018.01.049.
- [37] Marie PJ, Ammann P, Boivin G, Rey C. Mechanisms of Action and Therapeutic Potential of Strontium in Bone. *Calcif Tissue Res*. 2001;**69**:121. doi:10.1007/s002230010055.
- [38] Mondal S, Dorozhkin S, Pal U. Recent progress on fabrication and drug delivery applications of nanostructured hydroxyapatite. *Wiley Interdiscip Rev Nanomed Nanobiotechnol*. 2018;**10**(4). doi:10.1002/wnan.1504.
- [39] Loca D, Locs J, Salma K, Gulbis J, Salma I, Berzina-Cimdina L. Porous Hydroxyapatite Bioceramic Scaffolds for Drug Delivery and Bone Regeneration. *IOP Conf Ser: Mater Sci Eng*. 2011;**18**:192019. doi:10.1088/1757-899x/18/19/192019.
- [40] Ammann P, Shen V, Robin B, Mauras Y, Bonjour J, Rizzoli R. Strontium Ranelate Improves Bone Resistance by Increasing Bone Mass and Improving Architecture in Intact Female Rats. *J Bone Miner Res*. 2004;**19**(12):2012. doi:10.1359/jbmr.040906.

- [41] Pemmer B, Roschger A, Wastl A, Hofstaetter JG, Wobrauschek P, Simon R, Thaler HW, Roschger P, Klaushofer K, Strelia C. Spatial distribution of the trace elements zinc, strontium and lead in human bone tissue. *Bone*. 2013;**57**(1):184. doi:10.1016/j.bone.2013.07.038.
- [42] Barneo-Caragol C, Martínez-Morillo E, Rodríguez-González S, Lequerica-Fernández P, Vega-Naredo I, Álvarez Menéndez F. Strontium and oxidative stress in normal pregnancy. *J Trace Elem Med Biol*. 2018;**45**:57. doi:10.1016/j.jtemb.2017.09.021.
- [43] Marie PJ, Felsenberg D, Brandi ML. How strontium ranelate, via opposite effects on bone resorption and formation, prevents osteoporosis. *Osteoporos Int*. 2010;**22**(6):1659. doi:10.1007/s00198-010-1369-0.
- [44] Boivin G, Deloffre P, Perrat B, Panczer G, Boudeulle M, Mauras Y, Allain P, Tsouderos Y, Meunier PJ. Strontium distribution and interactions with bone mineral in monkey iliac bone after strontium salt (S12911) administration. *J Bone Miner Res*. 2009;**11**:1302. doi:10.1002/jbmr.5650110915.
- [45] Miguel FB, Barbosa Júnior AA, Paula FL, Barreto IC, Goissis G, Rosa FP. Regeneration of critical bone defects with anionic collagen matrix as scaffolds. *J Mater Sci Mater Med*. 2013;**24**(11):2567. doi:10.1007/s10856-013-4980-8.
- [46] Ribeiro IIA, Barbosa Junior AA, Rossi AM, Almeida RS, Miguel FB, Rosa FP. Strontium-containing nanostructured hydroxyapatite microspheres for bone regeneration. *Res Soc Dev*. 2023;**12**(4). doi:10.33448/rsd-v12i4.41222.
- [47] Anderson JM, Rodriguez A, Chang DT. Foreign body reaction to biomaterials. *Semin Immunol*. 2008;**20**(2):86. doi:10.1016/j.smim.2007.11.004.
- [48] Klopfleisch R. Macrophage reaction against biomaterials in the mouse model – Phenotypes, functions and markers. *Acta Biomater*. 2016;**43**:3. doi:10.1016/j.actbio.2016.07.003.
- (Rec. 17/07/2023, Rev. 16/10/2023, Ac. 01/12/2023) (AE: H. N. Yoshimura)

